

# Melt Production Rates in Mantle Plumes

Robert S. White

*Phil. Trans. R. Soc. Lond. A* 1993 **342**, 137-153

doi: 10.1098/rsta.1993.0010

## Email alerting service

Receive free email alerts when new articles cite this article - sign up in the box at the top right-hand corner of the article or click [here](#)

To subscribe to *Phil. Trans. R. Soc. Lond. A* go to:  
<http://rsta.royalsocietypublishing.org/subscriptions>

# Melt production rates in mantle plumes

BY ROBERT S. WHITE

*Bullard Laboratories, Madingley Road, Cambridge CB3 0EZ, U.K.*

I calculate the melt production rates for mantle plumes lying beneath oceanic lithosphere from the crustal thickening measured by using seismics and from the volume of the overlying ridge. Observed melt production rates are higher where the lithosphere is thinner, in accord with theoretical predictions of the processes of decompression melting in convective plumes. The productivity of mantle plumes, and in particular that of the Hawaiian plume, is shown to vary on timescales of a few tens of millions of years. This can be explained by variations in the temperature and flow rate of the plumes. The trace of the Réunion plume shows a marked drop in melt production over the 30 Ma following generation of the Deccan flood basalts, which reflects a decrease in the plume temperature from the transient abnormally hot conditions associated with initiation of the plume.

## 1. Controls on decompression melting

Decompression melting of the mantle occurs within plumes where the mantle rises buoyantly until it is deflected by the overlying lithosphere, and beneath rifts where the thinning lithosphere allows the underlying mantle to well up. When rifting occurs above a mantle plume, extremely large volumes of melt may be generated rapidly, because abnormally hot mantle can decompress to shallow depths.

The rate of melt production is governed by the bulk composition of the mantle, the presence of volatiles or water, the temperature of the mantle, the lithospheric thickness, and the rate of decompression. Of these factors, the bulk composition of the mantle varies little, so does not cause variations in melt productivity. Though volatiles or water have a marked effect on melting in regions such as those above subduction zones, I assume that the melting beneath mid-ocean ridges and in mantle plumes is dry and use McKenzie & Bickle's (1988) method to calculate the volume of melt generated by decompression. I outline below the effect on melt production of variations in mantle temperature, lithospheric thickness, and decompression rate.

### (a) *Plume temperatures and shapes*

Mantle plumes arise as boundary layer instabilities from deep in the Earth, though it is not yet clear whether they arrive at the surface directly from the core–mantle interface, or from the upper–lower mantle boundary. They are not necessarily axisymmetric, though are often modelled as such for computational reasons (Courtney & White 1986; Watson & McKenzie 1991). Rising spoke-like or triple junction patterns may be common at their base, particularly if there is significant internal heating (Parsons & Richter 1981; Houseman 1990). In places rising sheets of mantle may reach the surface, the 750 km long Cameroon Line and the 450 km long Rodrigues Ridge being possible examples.

*Phil. Trans. R. Soc. Lond. A* (1993) **342**, 137–153

© 1993 The Royal Society

*Printed in Great Britain*

137

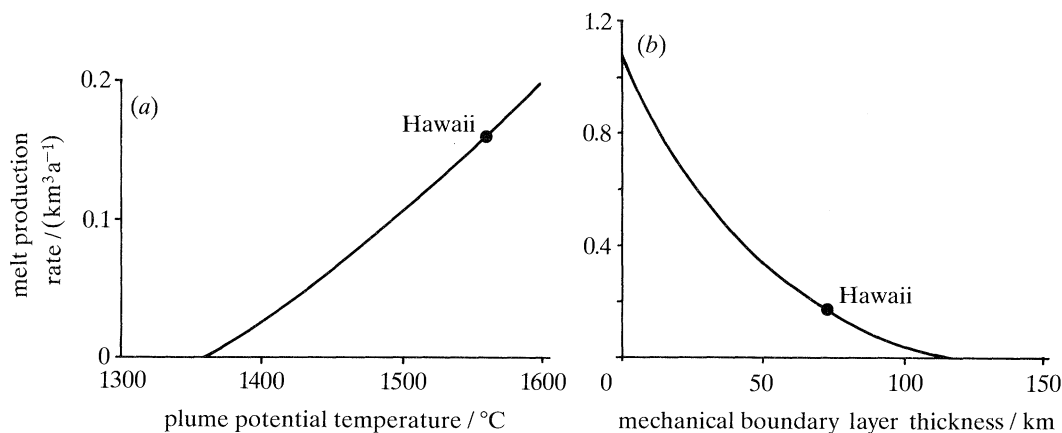


Figure 1. (a) Predicted variation of approximate melt production rate with potential temperature in the centre of the mantle plume; (b) predicted variation of melt production rate with thickness of the mechanical boundary layer. Both curves are from Watson & McKenzie's (1991) convection model for the present-day Hawaiian plume.

Plumes are not steady-state features. From time to time old plumes die out and new ones start. The mass flux and temperature of a new plume is higher than the subsequent flow, and many flood basalt provinces appear to be associated with the transient conditions accompanying the initiation of new plumes (White & McKenzie 1989). Many plumes have been documented as active over periods of the order of 100 Ma, but the difficulty of tracing them beneath continental lithosphere makes it uncertain whether any individual plumes have survived as long as 200 Ma.

The temperature within a plume can be estimated from the uplift and geoid anomaly it causes, by the increase in heat flow through the overlying seafloor, and by the rate of production and composition of the igneous rock it generates. Temperatures in mantle plumes are typically 250–300  $^{\circ}C$  above normal.

Watson & McKenzie (1991) show that although the average degree of melting beneath Hawaii is less than 7%, large volumes of melt are generated because the plume continually cycles mantle through the melting region. Figure 1a shows the approximate variation with temperature of melt production for models of the Hawaiian plume. A plume could exist beneath Hawaii with an excess temperature nearly 100  $^{\circ}C$  above the normal mantle temperature of 1280  $^{\circ}C$ , yet still produce negligible melt because the base of the lithosphere would prevent the convecting mantle rising sufficiently shallow to cross the solidus.

#### (b) Lithospheric thickness

Thick lithosphere prevents melting in plumes by limiting the decompression that can occur. In the Hoggar plume, for example, little melt is produced even though the plume causes regional uplift of about 1 km (Crough 1981). Conversely, thin lithosphere allows considerable melting in plumes.

Removal of melt reduces the density of the residual mantle (Oxburgh & Parmentier 1977; Bickle 1986). For slow-moving plates it is possible that depleted mantle accumulating above a plume may limit the vertical rise of the plume, thus reducing the amount of decompression melting that occurs. Conversely, heat conduction from a plume decreases the thickness of the overlying lithosphere, allowing increased decompression melting. The maximum lithospheric thinning from

heat conduction is less than 10% (Courtney & White 1986; Watson & McKenzie 1991). Neither of these effects is large, and they work in opposite directions, so it is unlikely that they can be detected in the geological record.

### (c) *Mantle plume flow rates*

Provided the lithosphere is sufficiently thin and the temperature sufficiently high for melting to occur, the melt production rate in plumes beneath intact plates is directly proportional to the mantle flow rate.

Beneath rifts away from hotspots, the mantle decompresses as it moves upward. For rapid stretching the heat loss by conduction can be ignored, and the total volume of melt generated by decompression depends only on the initial entropy and the amount of lithospheric thinning. At oceanic rifts, heat loss by conduction only causes a measurable decrease in the volume of melt spreading rates lower than  $20 \text{ mm a}^{-1}$  (White 1992).

Where a rift lies above a plume, as in many flood basalt provinces, the melt production depends on both the rate of stretching and on the mantle flow in the plume. At present these interactions are too complex to model satisfactorily. But it is likely that melting in many flood basalt provinces is controlled primarily by the rate of lithospheric rifting, because the melt production rates are so high (typically  $5\text{--}10 \text{ km}^3 \text{ a}^{-1}$ ) and the duration of the main igneous phase so short (typically  $0.5\text{--}2 \text{ Ma}$ ), that they can be explained only by rapid and widespread decompression.

## 2. Melt distribution in the crust

Less than 1%, and possibly as little as 0.1%, of the melt remains in the source mantle region. The melt moving upwards is distributed as surface flows, as dykes and sills within the mid-crust, or as massive underplated or heavily intruded regions in the lower crust.

### (a) *Surface flows*

Basaltic rocks can flow remarkably large distances. For example, subaerial flows in the Columbia River Basalt Group can be traced more than 750 km from the feeder dykes, with some flows exceeding  $2000 \text{ km}^3$  and probably approaching  $3000 \text{ km}^3$  in volume (Tolan *et al.* 1989). Underwater basaltic flows extend up to 60 km across a smooth sedimented surface in the northeast Pacific (Davis 1982). Where melt supply was unusually high, as in the Nauru Basin, western Pacific, huge flows similar to those found in subaerial flood basalts have been identified (Saunders 1985). They probably originated from the mantle plume volcanism presumed to have built the adjacent Ontong-Java Plateau (Tarduno *et al.* 1991; White *et al.* 1992).

Although flood basalts produce sufficient melt to feed enormous flows, both subaerial and submarine, the melt production rates from plumes beneath intact plates are much lower and individual eruptions are frequent and relatively small. The lava from oceanic volcanoes does not generally flow far underwater from the source. The flexural moat surrounding large oceanic volcanoes also restricts the outward movement of basaltic flows.

### (b) *Dyke intrusion*

Lateral dyke propagation is controlled mainly by a balance between viscous and buoyancy forces in the molten rock, with the strength of the medium through which the dyke moves affecting only the structure near the advancing tip (Lister 1990; Lister & Kerr 1991). Provided the melt supply is sufficiently large, basaltic dykes can

flow hundreds of kilometres laterally in continental crust. For example, the 1.27 Ga Mackenzie dykes extend 1500 km through the Archaean shield at mid-crustal levels. They were emplaced contemporaneously with the Akalulia and Coppermine River flood basalts, and appear to have been generated following rifting above a mantle plume in a similar manner to younger flood basalt provinces (LeCheminant & Heaman 1989). So we might expect similar dyking to occur in more recent flood basalt provinces, although it is often obscured by the basaltic cover. Only where this has been eroded off, can the dykes be readily seen.

Large dykes may propagate laterally less easily through oceanic than continental crust. Although it is almost impossible to determine whether dyke swarms are present in oceanic crust, the crustal thickening beneath hotspot islands appears to be localized above the plume. This suggests that there has been little lateral melt transportation, in contrast to continental settings where long-term uplift beneath flood basalts provides evidence of considerable crustal thickening and lateral melt movement (McKenzie 1984; Cox 1992). Around the Hawaiian plume, for example, Lindwall (1988) shows from seismics that the crust as close as 300 km to Hawaii is no thicker than normal oceanic crust, and Helmberger & Morris (1970) demonstrate the same on a profile 350 km from Hawaii. Seismic and gravity profiles across other volcanic ridges give similar results: there are abrupt decreases in crustal thickness on the margin of Iceland (Gebrande *et al.* 1980; Ritzert & Jacoby 1985); across the edge of the Madagascar Ridge (Sinha *et al.* 1981); and across the flanks of the Chagos-Laccadive Ridge (Francis & Shor 1966).

Dykes may propagate less easily through oceanic than through continental crust because the basaltic melt generated in mantle plumes is similar in composition to that of the oceanic crust through which it intrudes, and so has a similar density. Furthermore, oceanic crust is only about 20% the thickness of continental crust. Both factors mean that the level of neutral buoyancy is shallower in oceanic than in continental crust and much of the melt probably extrudes before it has the opportunity to migrate significant distances laterally.

### (c) *Underplating and lower crustal intrusion*

The evolved, uniform composition of tholeiitic flood basalts and of the majority of ocean island volcanics suggests that fractionation within or below the crust has left considerable volumes of residual igneous rock at depth (Cox 1980, 1992). When solidified in the lower crust the primary melts from plumes produce rocks with high seismic velocities and densities. Such rocks are found beneath volcanic rifted continental margins (White & McKenzie 1989; White 1992), and beneath intra-plate volcanic ridges (Sinha *et al.* 1981; Watts *et al.* 1985a; Zucca *et al.* 1982; ten Brink & Brocher 1987). Sometimes the primary lavas reach the surface without fractionating, as do the extensive picrites of the Lebombo monocline in the Karoo Province. However, more commonly they are trapped in the lower crust by their greater density, and can only rise to the surface when the density of the melt has been lowered by fractionation of olivine crystals (Stolper & Walker 1980). This explains both the relatively uniform composition of most tholeiitic basalts in flood basalts and ocean islands, and also the presence of large underplated igneous volumes.

The percentage of the melt emplaced in the lower continental crust is much greater than in oceanic crust. The main reason for this is probably the reduced density of continental crust, which makes it harder for the melts to rise through it than through the higher density oceanic crust. Furthermore, the melting temperature of the



continental crust may be as low as 600 °C, so the large quantities of melt at temperatures greater than 1200 °C that are injected into continental crust rapidly melt it and thus generate an even more effective density trap. The density and melting temperatures of oceanic crust are higher than those for continental crust, so it does not form such a good density trap.

Seismic studies suggest that 60–80 % of the melt is underplated on volcanic continental margins, but that much less is underplated beneath ocean islands. Under the Hawaiian Islands, for example, Watts *et al.* (1985*b*) and ten Brink & Brocher (1988) suggest from seismics that only about 40 % of the igneous melt is underplated, while Lindwall (1988) re-interpreted one of the same profiles to suggest that less than 15 % of the melt is underplated. In part the different estimates for the Hawaiian Islands highlight the ambiguity in interpreting lower crustal velocities, as either original oceanic crust or as newly intruded igneous rock. Nevertheless it is clear that a far smaller proportion of the melt is underplated beneath oceanic crust than beneath continental crust.

### 3. Melt production rates in mantle plumes

The melt emplacement rate in the crust varies on several timescales. From days to hundreds of years, the rates reflect processes at crustal levels as magma chambers inflate and are emptied. Up to a few millions of years the rates are governed largely by the lithosphere as melt rises through it from the underlying mantle. Many hotspots produce chains of individual islands or seamounts as melt is focused into one or more volcanoes, before jumping on to a new location. For example, over 100 separate volcanic centres exist along the 5700 km long Hawaiian-Emperor chain (Bargar & Jackson 1974). This focusing is probably caused by the rigid lithosphere and the necessity to open conduits through it for the passage of melt.

I am here concerned with longer term changes in the behaviour of mantle plumes. By averaging the rates measured at crustal levels over periods of about 10 Ma, I smooth out the fluctuations caused by solitary waves in the mantle, or by the control exerted by the lithosphere and crust.

#### (a) Estimation of melt production rates

Melt production rates are best estimated by using seismics to define the crustal thickness. I here consider plumes beneath oceanic plates because the thickness of the pre-existing crust is well known and varies little from 7 km away from obvious tectonic structures such as fracture zones (White *et al.* 1992). The measured crustal thickening can therefore be attributed to new igneous addition, and includes both extrusive and intrusive components.

The only seismic profiles across volcanic ridges modelled with synthetic seismograms are from the Hawaiian Ridge (Lindwall 1988), the Madagascar Ridge (Sinha 1981) and Kerguelen Plateau (Recq *et al.* 1990). However, older profiles interpreted using slope-intercept solutions are more widespread and still give an indication of the crustal thickness provided allowance is made for the likelihood that the crustal thicknesses are about 20 % too small because of the assumption of plane layers rather than the more likely velocity gradients (White *et al.* 1992; see also plane-layer versus synthetic seismogram interpretations of the Madagascar Ridge in Sinha *et al.* (1981)).

Even using results only from volcanic chains with seismic control, we must still

extrapolate from the few locations where the thicknesses are known. For this, I assume local Airy compensation and estimate the total igneous thickness from the volume of the ridge above a base level, calculated by digitizing bathymetric contours. This is similar to Schubert & Sandwell's (1989) approach, except that they used  $15' \times 15'$  bathymetric averages and a different method for defining the excess volume of the volcanic ridges.

There are two major uncertainties in calculating the excess volume of a ridge, both of which arise from the difficulty of defining the base level. An active plume causes up to 1–2 km uplift and affects a region of up to 2000 km diameter. After a plume has moved away, it takes 50–100 Ma for the excess heat to conduct through the lithosphere, and for the bathymetry to subside to its pre-plume depth. Superimposed on this is permanent uplift caused by the decreased density of partly depleted mantle, which remains even after the plume has gone. Both mechanisms elevate the seafloor around volcanic ridges above the normal oceanic subsidence curve.

I here define the boundary of a volcanic ridge as the location of the break in slope from the gentle, long-wavelength swell, to the steep volcanic edifice. Where the lower part of the ridge has been buried in thick sediments, I extrapolate downward to a deeper base level representing the top of the igneous basement rather than using the present seafloor.

The total igneous volume is calculated assuming Airy isostasy, with a mean density difference of  $0.3 \text{ Mg m}^{-3}$  between the crust and mantle. Several approximations are involved in this. The density of the underplated region is probably greater than that of the extruded volcanics, which would lead to a thicker crust than I calculate. However, the density of the depleted mantle is probably lower beneath the ridge than elsewhere, and if this were properly included, I would calculate a thinner crust. Since the densities are not well known, my simple assumption of a single density difference is reasonable, and is in any case probably not far wrong because these two sources of error work in opposite directions. Where the volcanic ridge was constructed on very young lithosphere, the assumption of local Airy isostasy is better than where the ridge was emplaced on older lithosphere and part of the load is supported over a wide area (e.g. Hawaiian Ridge (Watts & ten Brink 1989)). Nevertheless, I have confidence that this straightforward approach gives useful answers by ensuring that the total igneous volume predicted by this method is in agreement with the total volume determined from seismic measurements, at the locations where both methods are available.

### (b) *Melt variation with time: the Hawaiian plume*

For the past 35 Ma the Hawaiian plume has lain beneath oceanic lithosphere some 80 Ma older than itself (figure 2, top). This removes lithospheric thickness variations as a possible control on the melt production rate and leaves variations in the temperature and flow rate of the plume itself as the major variable factor. The present melt production rate measured from seismics near Oahu (Watts *et al.* 1985*b*) is  $0.14\text{--}0.18 \text{ km}^3 \text{ a}^{-1}$  (square symbols, figure 2), in agreement with the 10 Ma running average calculated assuming Airy isostasy.

Over the past 35 Ma the melt production of the Hawaiian plume has increased steadily by an order of magnitude. If the plume flow rate has remained unchanged over that period, a temperature increase of about  $150^\circ$  at the centre would explain this increase (figure 2). Alternatively, if the flow rate of the plume has increased over the past 35 Ma then a smaller change in plume temperature would be required to

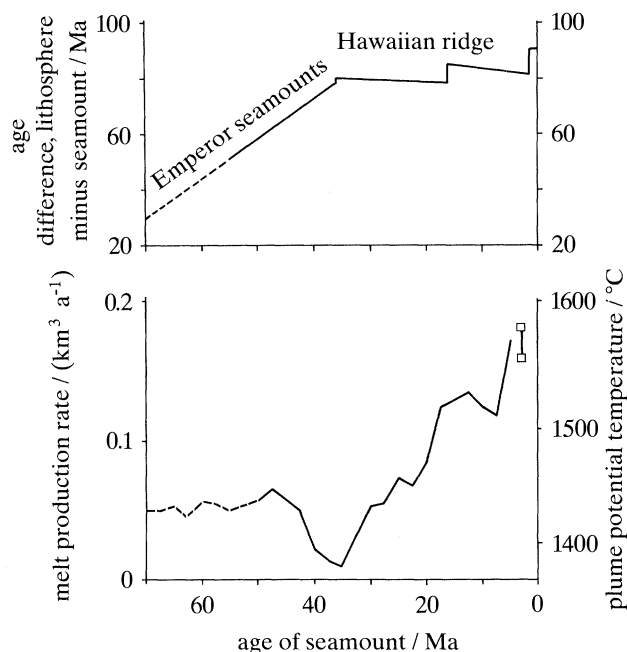


Figure 2. Lower diagram shows variation of melt production rate (left-hand scale) with age along the Hawaiian-Emperor seamount chain. Total melt rate is calculated from the volumes above the break in slope at the seafloor of individual shield volcanoes (Bargar & Jackson 1974), extrapolated to include underplated region by assuming local Airy isostasy. A running average of 10 Ma has been calculated every 2.5 Ma along the seamount chain, omitting the currently active volcanoes of Mauna Loa, Kilauea and Loihi. Open squares show the range in mean igneous production rate from a cross-section based on seismics near Oahu from Watts *et al.* (1985*b*), with the range indicating different assumptions of how much igneous material has been eroded off into the moat adjacent to the islands. Right-hand scale shows approximate variations in the potential temperature at the centre of the plume which would account for the variations in melt production rate over the period 35–0 Ma, assuming that the flow in the mantle plume remained unchanged from that deduced by Watson & McKenzie (1991) for the present day (see figure 1*a*). Top diagram shows age of the lithosphere at the time of emplacement of seamounts along the Hawaiian-Emperor chain (after Clague & Dalrymple 1987). During 35–0 Ma the plume has remained beneath lithosphere consistently 80 Ma older than the seamounts, while before 35 Ma, the older the seamounts, the younger the lithosphere at the time of emplacement.

explain the increased melt production. In either case it is clear that the vigour of the mantle plume has increased over a timescale of 35 Ma, making Hawaii at the present day the most active intra-plate volcano in the world.

Over the period 50–35 Ma the melt rate was decreasing to the low at 35 Ma (figure 2). At 50 Ma the lithosphere on which the seamounts were being emplaced was some 20 Ma younger than at 35 Ma (figure 2, top), but the concomitant increase in lithospheric thickness from 50–35 Ma is too small to explain most of the melt production rate drop over the same period.

Melt production was approximately constant during the period 70–50 Ma. However, this oldest section of the Emperor Seamounts is also partly buried by terrigenous sediments so it is likely that the total volumes of the seamounts are underestimated. Correction for this would increase the melt production rates along the oldest remaining section of the volcanic chain.

I conclude that changes in the plume temperature and flow, over timescales of a



few tens of Ma are responsible for the long-term changes in melt production recorded along the Emperor-Hawaiian seamount chain.

(c) *Melt variation with time in the Réunion plume*

The Réunion plume spent the first 30 Ma of its recorded history beneath very young lithosphere, so it provides a contrast to the Hawaiian plume. From the time of the Deccan flood basalts at 66 Ma, probably coinciding with initiation of the Réunion plume, until about 35 Ma when it crossed the Central Indian Ridge, the plume lay close to the spreading ridge (Schlich 1982; Royer *et al.* 1989) and generated the huge volcanic ridge beneath the Laccadives, the Maldives, Chagos Bank and Saya da Malha Bank. Volcanic dates from borehole samples show a progression along the chain, with southern Chagos Bank and Saya da Malha Bank being formed at the same time, but subsequently split by continued seafloor spreading along the Central Indian Ridge (Duncan & Hargraves 1990).

Airy isostatic balances of the excess ridge topography indicate crustal thickening of about 20 km, in accord with sparse seismic refraction measurements reported by Francis & Shor (1966). Their reversed refraction line 4–5 in a channel between the Maldive and Chagos archipelagos did not reach Moho, despite a 100 km line length, from which they conclude that the Moho is unlikely to be shallower than 20 km. They also recorded a mid-crustal refractor with a velocity higher than  $7.1 \text{ km s}^{-1}$ , which is typical of the underplating found elsewhere under volcanic ridges. Further north, a profile between the Laccadives and Maldives recorded Moho at just over 17 km depth: taking account of velocity gradients and the probably higher velocity of material in the lower crust would increase this to well over 20 km.

Melt production over 66–35 Ma shows a steady decrease from the peak rates in the Deccan (figure 3). These rates are an order of magnitude higher than those of the Hawaiian-Emperor chain, reflecting the thinner lithosphere and the hotter mantle in the initiating plume. The Indian plate was moving northwards rapidly with respect to the Réunion plume during this period, allowing the melt to migrate upward to generate a thick igneous ridge, which reached well above sea-level. Since the plume lay under young lithosphere during the period 64–35 Ma, the decrease in melt production is probably due to decreasing temperature and flow rate in the plume following the peak as it initiated. The timescale of several tens of millions of years over which this occurred is similar to the timescale over which the Hawaiian plume changes have taken place.

As the plume passed beneath older lithosphere south of the Central Indian Ridge, the melt production continued to decrease, building first a series of smaller ridges, including Nazareth and Cargados-Carajos Banks, and then individual volcanic shields like Mauritius and Réunion, similar to the isolated seamounts generated along the Hawaiian-Emperor chain. Correction of the melt production rates to those that would have been generated under 20 km thick lithosphere comparable to that beneath the Chagos-Laccadive Ridge, flattens out the rate of decline in the melting (open symbols, figure 3). The vigour of the present plume is now comparable to that of mature plumes elsewhere.

(d) *Melt variation with lithosphere thickness*

Variations in melting caused by changes in the plume temperature are superimposed on the control exerted by the lithospheric thickness. The major plumes show a decrease in melt production rates with increasing lithospheric thickness

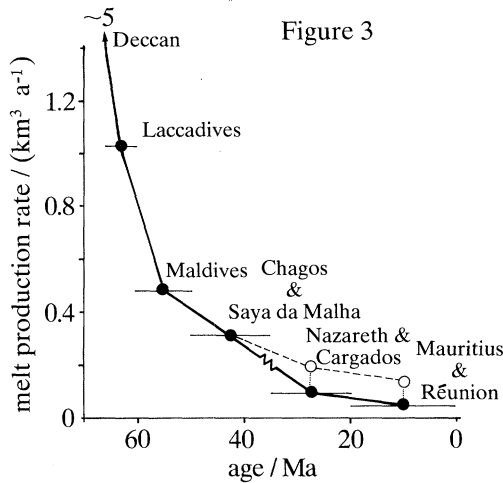


Figure 3

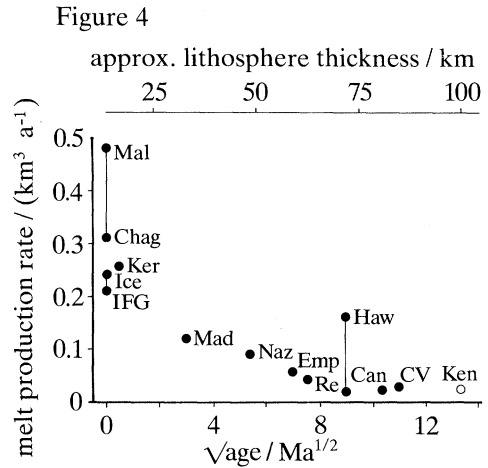


Figure 4

Figure 3. Variation of melt production rate with age along the trace of the Réunion plume, calculated from the bathymetric expression of the volcanic ridge, assuming Airy isostatic equilibrium and with thickness control from seismic refraction experiments of Francis & Shor (1966). Volcanic ages are from Duncan & Hargraves (1990), with horizontal bars showing period over which the rate is averaged. From the time of the Deccan flood basalts at 66 Ma until approximately 35 Ma when the plume crossed the spreading axis of the Central Indian Ridge, the plume remained beneath young lithosphere. Since 35 Ma the plume has migrated beneath progressively older lithosphere with Réunion island currently being built on 67 Ma oceanic crust. Open circles are an approximate correction of the measured rates back to those that would be expected beneath 20 km thick lithosphere to make it comparable to the rates from 66–35 Ma, using the melt rate against lithosphere thickness curve shown in figure 1*b*.

Figure 4. Melt production rates in mantle plumes (see table 1 for key) against the square root of the age of the oceanic lithosphere beneath which they lay. Approximate lithospheric thickness at the time of emplacement is shown along the top. The Kenyan plume (open symbol) lies beneath continental lithosphere about 100 km thick (see text for details). Note that for any given lithospheric thickness, variations in the plume temperature or in the vigour of mantle flow may cause variations in the melt production rate, such as are indicated for the Hawaiian Chain, for Iceland and the Iceland–Faeroes–Greenland Ridge, and for the Chagos and Maldiva Ridges. Compare the general trend in observed rates with those predicted from convection modelling in figure 1*b*.

(figure 4 and table 1), similar to that predicted by simple convection models of plumes (figure 1*b*). Where the variations with age are known, as in the cases of the Hawaiian and Réunion plumes, I show the range on figure 4. Elsewhere I average across several tens of Ma to obtain a long-term mean.

#### (i) *The Iceland plume*

Igneous activity on the rifted continental margins of the northern North Atlantic shows a peak at break-up, caused by the transient abnormally hot mantle in the newly initiated Iceland plume. Igneous thickness estimates on the rifted margin and in the adjacent oceanic basin suggest that the mantle temperature dropped by more than 50 °C during the first 10 Ma following arrival of the new plume (Morgan *et al.* 1989; White 1992).

Oceanic crust adjacent to the Iceland plume averages  $10.3 \pm 1.7$  km thick (White 1992). Minor variations in melt productivity are suggested by V-shaped discontinuities that propagate across the Irminger and Iceland Basins, and by the appearance of seaward-dipping reflectors on the Kolbeinsy Ridge between 20–10 Ma.

Table 1. *Melt production rates above mantle plumes*

(Table shows melt production rates in excess of the 7 km of melt which generates normal thickness oceanic crust. The age of plume volcanism is the range used to calculate the melt productivity rate shown in the last column.)

abbreviation on figure 4	plume trace	age of plume volcanism/Ma	melt rate $\text{km}^3 \text{a}^{-1}$
Can	Canaries	60–0	0.02
Chag	Chagos plus Saya-da-Malha Banks	50–35	0.31
CV	Cape Verdes	25–0	0.03
Emp	Emperor Seamounts	60–40	0.06
Haw	Hawaiian Ridge	40–0	0.03–0.16
Ice	Iceland	35–0	0.24
IFG	Iceland–Faeroes–Greenland Ridges	55–35	0.21
Ken	Kenyan Rift	23–0	0.02
Ker	North Kerguelen plus Broken Ridge plus 90E Ridge	80–38	0.25
Lacc	Laccadive Ridge	66–60.5	1.03
Mad	Northern Madagascar Ridge	120–95	0.12
Mal	Maldives Ridge	60.5–50	0.48
Naz	Nazareth Ridge plus Cargados–Carajos Bank	35–20	0.09
Re	Réunion and Mauritius	20–0	0.04

The Iceland–Faeroe Ridge generated directly above the plume is 30–35 km thick (Bott & Gunnarsson 1980). Assuming Airy isostasy, and with an allowance for an equal volume of igneous rocks in the largely unexplored Iceland–Greenland Ridge, this suggests an excess melt production rate above that in the adjacent oceanic spreading centre of  $0.21 \text{ km}^3 \text{a}^{-1}$  during 55–35 Ma. However, as Bott & Gunnarsson (1980) comment, this thickness estimate is too small if there are high velocities or velocity gradients in the lower crust. The most probable rate, after allowance for the likelihood of increased velocities in the lower crust, is about  $0.26 \text{ km}^3 \text{a}^{-1}$ . There is some indication that the crust is thinner towards the younger, northwestern end, which would indicate gradually decreasing temperatures with time.

Beneath Iceland itself, the crustal thickness is uncertain because normal mantle velocities are not reached even by a depth of 50 km. Seismic velocities increase from about  $7.0 \text{ km s}^{-1}$  at 15 km depth to  $7.6 \text{ km s}^{-1}$  at 50 km depth, with a band of higher velocity layers at about 30 km (Gebrande *et al.* 1980). These velocities and the absence of a mature Moho are similar to the structure found beneath many active oceanic spreading centres, with the most likely explanation being that they are caused by enhanced temperatures and the presence of melt. The maximum crustal thickness is probably about 30 km, corresponding to the higher velocity lenses at that depth, and the minimum crustal thickness is around 20–24 km, corresponding to a reflector recorded at that depth in the south of Iceland (Bjarnason *et al.* 1992). With the present extent of the rift beneath Iceland and the full spreading rate of  $19 \text{ mm a}^{-1}$ , this gives an excess melt production rate of  $0.12\text{--}0.24 \text{ km}^3 \text{a}^{-1}$  above that beneath the adjacent Reykjanes Ridges caused by passive upwelling. I favour the higher rate of  $0.24 \text{ km}^3 \text{a}^{-1}$ , which is in agreement with the excess volume for the past 35 Ma calculated assuming Airy compensation by Schubert & Sandwell (1989), because this agrees well with the rate from the Iceland–Faeroes Ridge and there is

no evidence from crustal thicknesses on the adjacent oceanic crust of a marked decrease in mantle temperatures over the past 50 Ma.

(ii) *Madagascar Rise*

The Madagascar Rise extends 1300 km southwards from Madagascar. It marks the trace of a plume which was responsible for the Upper Cretaceous Madagascar flood basalts formed as Gondwana broke up (Mahoney *et al.* 1991), and which generated the recent volcanism of Prince Edwards and Marion Islands, and possibly also of Crozet Island. The northern Madagascar Rise, with a water depth of 2–3 km, and 0.5–1.0 km of undisturbed sediments, was formed as the plume lay beneath newly created oceanic lithosphere perhaps 10 Ma old. Subsequently, the plume crossed the Southwest Indian Ridge, and its track thereafter is uncertain. Melt production increased as the plume crossed the zero-age lithosphere beneath the spreading centre, as is indicated by the thicker ridge in the southern part of the Madagascar Rise, topped by Walters Shoal which reaches to within 20 m of the sea surface.

I here consider melt production in just the northern Madagascar Rise, where the crustal structure is well constrained by seismics modelled by using synthetic seismograms (Sinha *et al.* 1981). These show a 20–25 km thick crust, with an 8 km thick lower crustal layer of about  $7.6 \text{ km s}^{-1}$ , representing the underplated more mafic region. Plume production rates calculated from both the seismic cross section and from gravity modelling assuming Airy compensation are about  $0.12 \text{ km}^3 \text{ a}^{-1}$ .

(iii) *Canary plume*

For the past 60 Ma the plume which now lies beneath the Canary Islands has traversed beneath Mesozoic oceanic lithosphere in the eastern Central Atlantic some 110 Ma older than the plume. Holik & Rabinowitz (1992) interpret a 150–200 km wide zone of chaotic reflectors within the Cretaceous sediments as extrusive volcanics averaging just over 1 km thick. In the same area at the base of the crust they report a 200 km wide, 1.0–3.5 km thick high-velocity ( $7.1\text{--}7.4 \text{ km s}^{-1}$ ) layer interpreted as underplated igneous rocks. These igneous rocks added to the crust lie along the track of the Canary plume and coincide with elevated subsidence curves consistent with the uplift caused by a plume. The melt production rate during the period 60–50 Ma calculated from the inferred igneous thicknesses is  $0.01\text{--}0.02 \text{ km}^3 \text{ a}^{-1}$ .

The Canary Islands themselves represent the most recent activity of the plume, with ages decreasing irregularly from the east to the west, consistent with the motion of the plate. Many of the islands exhibit a long (more than 20 Ma) magmatic history, a result of the slow motion of the plate. They are composed dominantly of shield-building basalts with local tholeiites, a consequence of the thick lithosphere and the resulting small degrees of mantle melting. Seismic refraction results from beneath the islands have not been modelled with synthetic seismograms, but suggest that the Moho is at least 17 km deep. A 3 km thick basal layer with a velocity of  $7.1\text{--}7.5 \text{ km s}^{-1}$  (Bosshard & Macfarlane 1970) probably represents underplated igneous rocks. Basal velocities of  $7.4 \text{ km s}^{-1}$  beneath Lanzarote and Fuerteventura were interpreted by Banda *et al.* (1981) as mantle, but may also represent intruded igneous rocks. From seismic and gravity data the average rate of accreting underplated igneous rock is  $0.01 \text{ km}^3 \text{ a}^{-1}$ , and the rate of extrusion in island building is a little under  $0.01 \text{ km}^3 \text{ a}^{-1}$  (Schmincke 1982), giving a total melt production rate of  $0.02 \text{ km}^3 \text{ a}^{-1}$ .



(iv) *Cape Verde plume*

Like the Canaries, the Cape Verde islands were generated by a plume beneath late Jurassic oceanic lithosphere. The main igneous activity has occurred over the past 25 Ma, but the slow relative motion of only  $9 \text{ mm a}^{-1}$  between the African plate and the plume means that there is no clear age progression in the islands, other than a general younging towards the west, and that individual islands have been active for long periods. The 8 m geoid anomaly, 2 km uplift and 25% increase in heat flow beneath the islands have been modelled by convection in a mantle plume (Courtney & White 1986). Seismic refraction profiles yield an average crustal thickness of 11.4 km beneath the archipelago (Dash *et al.* 1976). Since these were interpreted by using the slope-intercept method, the true crustal thickness is probably about 20% greater or approximately 14 km. Across the archipelago, this yields a melt production rate in the mantle plume of  $0.03 \text{ km}^3 \text{ a}^{-1}$ , similar to that found for the Canaries.

(v) *Kenya plume*

The plume beneath Kenya has produced regional uplift (Ebinger *et al.* 1989) and volcanism in the Kenyan Rift over the past 30 Ma. Volcanism has been most active since the Miocene and I here consider only melt production rates during the last 23 Ma. The total igneous volume has to be estimated from the mapped volumes of extrusive basalt by allowing for fractional crystallization and calculating the amount of gabbro that is likely to be left in the lower crust: the volume of intrusives found in this way account for about 70% of the total igneous rock, which is consistent with the ratio of intrusive to extrusive rocks observed elsewhere in continental crust by using seismic methods. Excluding rhyolites, which are presumed to be crustal melts and therefore not directly from the mantle plume, and excluding hyperalkalic rocks in a volcanic chain to the west of the Kenyan Rift,  $212\,000 \text{ km}^3$  of melt was produced in the Miocene,  $166\,800 \text{ km}^3$  in the Pliocene and  $38\,400 \text{ km}^3$  in the Quaternary (Karson & Curtis 1989, and sources referenced therein). These yield an overall average melt production rate of just under  $0.02 \text{ km}^3 \text{ a}^{-1}$ , with a similar rate of  $0.02 \text{ km}^3 \text{ a}^{-1}$  in the Miocene and the Pliocene considered separately. There are indications of shorter-term variations in melting, with the rate dropping to about half in the last 2.5 Ma represented by the Quaternary, but being perhaps twice as high in the last half of the Pliocene (Williams 1972).

It is not easy to define the lithosphere thickness beneath the Kenyan Rift, although seismic reflection (Karson & Curtis 1989) and wide-angle refraction (Green *et al.* 1992; KRISP Working Party 1991) data indicate that crustal extension and thinning, and therefore by implication lithospheric thinning, has occurred. Karson & Curtis (1989) suggest that crustal extension has been less than 10% across the Kenyan Rift, and that much of the crustal thinning has been compensated by igneous intrusion from the plume. KRISP (1991) show that variable crustal thinning reaching 10–15 km has occurred within parts of the Kenyan Rift, and suggest that extension by between 10 and 35–40 km has occurred across different parts of the rift. Given the present rift valley width, this suggests local extension across the rift reaching 10–50%. If the original lithospheric thickness was 150 km, and stretching was by pure shear, then the lithosphere would be thinned beneath the rift to a minimum of about 100 km, so I take this as a representative thickness for plotting the Kenyan plume melt rate on figure 4. Note that Green *et al.* (1992) report the lithosphere–asthenosphere boundary as rising to depths of only 35–65 km beneath



the rift, but they use a definition for asthenosphere as mantle containing partial melt (which causes reduced seismic velocities). In considering the limits on decompression of rising material in a mantle plume it is the mechanically rigid layer which forms the lithospheric lid, irrespective of how much partial melt may be migrating through it, so Green *et al.*'s definition of very shallow asthenosphere is not appropriate for our purposes.

(vi) *Other plumes*

I have only shown on figure 4 results from those plumes where there is reasonably good control on the melt production rates. However, there are many other plumes where it is clear that the same dependence is found for melting as a function of lithospheric thickness. For example, the production rate from the Hoggar plume beneath unbroken, thick continental lithosphere is extremely low, while the nearby Afar plume beneath a major continental rift has produced flood basalts and a thick underplated region (White & McKenzie 1989).

In the South Atlantic, the Tristan plume lay beneath the spreading axis from 120–70 Ma creating the Rio Grande Rise and the eastern portion of the Walvis Ridge with crustal thickening of 8–15 km deduced from gravity measurements (Detrick & Watts 1979). From 70 Ma onwards the plume lay away from the spreading axis, and created a volcanic ridge on just the African plate, with reduced crustal thickening of 7–10 km. At present, Tristan da Cunha is some 450 km off the axis with much reduced melt productivity. So in this case, also, a progressive decrease in melting accompanies migration of the plume beneath thicker lithosphere.

There are also many other smaller plumes, such as the Saint Helena and Ascension plumes, which probably have lower temperatures or reduced mantle flow rates than the major plumes considered in this section, and which would therefore plot below the points shown on figure 4.

(e) *Melt variations with plate velocity*

There is a hint from my results that melt productivity is higher from mantle plumes beneath fast-moving plates than from those beneath slow-moving plates, although the sample size is insufficient to separate out conclusively this possible effect from temporal changes in mantle flow. For plumes beneath the ridge axes of slow-spreading oceans, the production of large quantities of melt itself thickens the overlying lithosphere by freezing to form new crust and hence serves to reduce further melt generation by reducing the amount of decompression possible. Furthermore, the reduced density of the residual mantle left after extraction of partial melt also tends to inhibit decompression of the underlying mantle plume on slow-spreading ridges.

In contrast, where the plume lies beneath a fast-moving plate, the plate continually sweeps away the thickened crust and residual mantle. In Watson & McKenzie's (1991) convection model of the Hawaiian plume the radial velocity of the asthenospheric mantle is about 70 mm a<sup>-1</sup> at a distance of 200 km from the plume centre, reducing to 40 mm a<sup>-1</sup> at 400 km distance. Since the Pacific plate is moving across the Hawaiian plume at a rate of about 100 mm a<sup>-1</sup> (Gripp & Gordon 1990) the plate velocity is higher than the horizontal outward flow of mantle from the plume so the plume moves progressively beneath fresh lithosphere. Although the Canary, Cape Verde and Réunion plumes lie beneath oceanic lithosphere of similar age to that beneath Hawaii, the overlying African plate is moving much more slowly than the

Pacific plate, at only 9–13 mm a<sup>-1</sup> (Gripp & Gordon 1990), and the melt production rates are much lower (figure 4). For the plumes beneath the African plate the horizontal mantle flow rates fed by the plume are always much higher than the plate velocity, so the centre of the plume where decompression melting occurs always lies beneath a region which has been thoroughly affected by radial flow from the plume for a long period before transit across the centre of the plume.

Similarly reduced melt productivity is apparent in plumes beneath very young slow-spreading ridges. The Chagos–Maldives–Laccadive Ridge was formed on very young oceanic crust, as was the Faeroe–Iceland–Greenland Ridge. But melt production rates were much greater in the Chagos–Maldives–Laccadive Ridge where the plates were moving rapidly (120 mm a<sup>-1</sup>) than in the Faeroes–Iceland–Greenland Ridge where the plates were moving only slowly (20 mm a<sup>-1</sup>).

#### (f) *Melt production in plumes beneath continental rifts*

Where plumes lie beneath continental rifts, high melt production rates occur, particularly if the rifting occurs during the transient thermal conditions accompanying initiation of a new plume (White & McKenzie 1989). The relationship between rifting and magmatism is complex: the presence of a plume provides significant uplift which fosters extension and rifting, but huge volumes of melt can only be generated very rapidly if the mantle can decompress to shallow depths beneath stretched and thinned lithosphere. The earliest igneous activity is likely to occur as soon as the plume impinges on the lithosphere, and before major rifting occurs, but the volumes of such melts are likely to be small. On the other hand, the bulk of the melt generated by mantle decompression will be produced before the onset of seafloor spreading proper, by which time the continental lithosphere has rifted fully. So if the oldest seafloor spreading anomaly or the date of opening of the new ocean is used as the age of rifting, then it will post-date the majority of the flood basalts. Unravelling this complex interaction between tectonics and magmatism requires better age control than exists at present in many flood basalt provinces.

It is, however, clear that massive outbursts of igneous activity can only result if there is thin lithosphere above a mantle plume, and preferably a newly initiated plume for maximum effect. The thin lithosphere may result from continental break-up, perhaps itself encouraged by the presence of a plume, or as in the case of the Ontong–Java Plateau, may result from the arrival of a plume beneath very young, and therefore thin oceanic lithosphere.

## 4. Conclusions

Magmatism resulting from mantle plumes is controlled primarily by the overlying lithospheric thickness. If the lithosphere is thick, little melt will be produced because insufficient decompression can occur. Where the lithosphere is thin, either because the plume lies beneath young oceanic lithosphere or beneath rifting continental or oceanic lithosphere, then large quantities of melt are produced by mantle decompression. The transient conditions accompanying the initiation of new plumes produce particularly large melt productivity. Variations in the temperature and flow rates of mature mantle plumes occur over timescales of several tens of Ma.

The rate at which the overlying plate moves with respect to a plume also appears to exert some control on the melt productivity. More melt is generated in plumes beneath fast-moving plates than in those beneath slow-moving plates, probably

because the fast-moving plate clears away the products of melting and the residual depleted mantle leaving the plume beneath pristine lithosphere.

Once melt has been generated in a plume it bleeds rapidly upward to the crust. It may then flow considerable distances laterally away from the source region, either as surface flows or as dykes at mid-crustal levels, provided the melt supply rates are sufficiently high to allow flow without freezing. Considerably more melt is underplated and travels laterally as sills or as dykes in continental crust than in oceanic crust. At the distal ends of dykes the melt may intrude at shallow levels or may feed local igneous centres. Therefore the final distribution of igneous rocks, and their history of fractionation and of crustal assimilation is likely to be far more complex than might be suggested by the relatively straightforward process of their generation by decompression melting in a plume or beneath a rift. A major key to understanding these relationships is good dating of the absolute ages and the rates of magmatism and of tectonic processes. Allied to these physical constraints, the geochemistry of the melts themselves provide evidence of the conditions under which the melt was generated (McKenzie & O'Nions 1991; Ellam 1991; White *et al.* 1992). The combination of knowledge of the rates and volumes of melt production with the geochemistry and petrology of the melts themselves is a powerful tool in understanding processes of melt generation in mantle plumes.

This work forms part of a study of the continental and oceanic lithosphere supported in part by the Natural Environment Research Council. Contribution number ES2849.

## References

- Banda, E., Danobeitia, J. J., Surinach, E. & Ansorge, J. 1981 Features of crustal structure under the Canary Islands. *Earth planet. Sci. Lett.* **55**, 11–24.
- Bargar, K. E. & Jackson, E. D. 1974 Calculated volumes of individual shield volcanoes along the Hawaiian-Emperor chain. *J. Res. U.S. Geol. Survey* **2**, 545–550.
- Bickle, M. J. 1986 Implications of melting for stabilisation of the lithosphere and heat loss in the Archaean. *Earth planet. Sci. Lett.* **80**, 314–324.
- Bjarnason, I. Th., Menke, W., Florenz, O. G. & Caress, D. 1992 Tomographic image of the spreading center in southern Iceland. *J. geophys. Res.* (Submitted.)
- Bosshard, E. & Macfarlane, D. J. 1970 Crustal structure of the western Canary Islands from seismic refraction and gravity data. *J. geophys. Res.* **75**, 4901–4918.
- Bott, M. H. P. & Gunnarsson, K. 1980 Crustal structure of the Iceland–Faeroe Ridge. *J. geophys.* **47**, 221–227.
- Campbell, S. M. & Griffiths, R. W. 1990 Implications of mantle plumes for the evolution of flood basalts. *Earth planet. Sci. Lett.* **99**, 79–93.
- Clague, D. A. & Dalrymple, G. B. 1987 The Hawaiian-Emperor volcanic chain. I. Geologic Evolution. In *Volcanism in Hawaii* (ed. R. W. Decker, T. L. Wright & P. M. Stauffer), pp. 5–50. US. Geological Survey Professional Paper 1350. Washington, D.C.: U.S. Govt Printing Office.
- Courtney, R. C. & White, R. S. 1986 Anomalous heat flow and geoid across the Cape Verde Rise: evidence for dynamic support from a thermal plume in the mantle. *Geophys. J. R. astr. Soc.* **87**, 815–867 and microfiche GJ 87/1.
- Cox, K. G. 1980 A model for flood basalt volcanism. *J. Petrol.* **21**, 629–650.
- Crough, S. T. 1981 Free-air gravity over the Hoggar Massif, north-western Africa: evidence for alteration of the lithosphere. *Tectonophysics*. **77**, 189–202.
- Dash, B. P., Ball, M. M., King, G. A., Butler, L. W. & Rona, P. A. 1976 Geophysical investigation of the Cape Verde archipelago. *J. geophys. Res.* **81**, 5249–5259.
- Davis, E. E. 1982 Evidence for extensive basalt flows on the sea floor. *Geol. Soc. Am. Bull.* **93**, 1023–1029.

- Detrick, R. S. & Watts, A. B. 1979 An analysis of isostasy in the world's oceans: three aseismic ridges. *J. geophys. Res.* **84**, 3637–3655.
- Duncan, R. A. & Hargraves, R. B. 1990  $^{40}\text{Ar}/^{39}\text{Ar}$  geochronology of basement rocks from the Mascarene Plateau, the Chagos Bank, and the Maldives Ridge. In *Proc. ODP, Sci. Results* (ed. R. A. Duncan *et al.*), vol. 115, pp. 43–52. College Station, Tx (Ocean Drilling Program).
- Ebinger, C. J., Bechtel, T. D., Forsyth, D. W. & Bowin, C. O. 1989 Effective elastic plate thickness beneath the East African and Afar Plateaus and dynamic compensation of the uplifts. *J. geophys. Res.* **94**, 2883–2901.
- Ellam, R. M. 1992 Lithospheric thickness as a control on basalt geochemistry. *Geology* **20**, 153–156.
- Francis, T. J. G. & Shor, G. G. 1966 Seismic refraction measurements in the northwest Indian Ocean. *J. geophys. Res.* **71**, 427–449.
- Gebrande, H., Miller, H. & Einarsson, P. 1980 Seismic structure of Iceland along RRISP-Profile I. *J. Geophys.* **47**, 239–249.
- Green, W. V., Achauer, U. & Meyer, R. P. 1991 A three-dimensional seismic image of the crust and upper mantle beneath the Kenya Rift. *Nature, Lond.* **354**, 199–203.
- Gripp, A. E. & Gordon, R. G. 1990 Current plate models relative to the hotspots incorporating the NUVEL-1 global plate motion model. *Geophys. Res. Lett.* **17**, 1109–1112.
- Helmberger, D. V. & Morris, G. B. 1970 A travel time and amplitude interpretation of a marine refraction profile: transformed shear waves. *Bull. seis. Soc. Am.* **60**, 593–600.
- Holik, J. S. & Rabinowitz, P. D. 1992 Effects of Canary hotspot volcanism on structure of oceanic crust off Morocco. *J. geophys. Res.* **96**, 12093–12067.
- Houseman, G. A. 1990 The thermal structure of mantle plumes: axisymmetric or triple-junction? *J. Geophys. Int.* **102**, 15–24.
- Karson, J. A. & Curtis, P. C. 1989 Tectonic and magmatic processes in the Eastern Branch of the East African Rift and implications for magmatically active continental rifts. *J. African Earth Sci.* **8**, 431–453.
- KRISP Working Group 1991 Structure of the Kenya Rift from seismic refraction. *Nature, Lond.* **325**, 239–242.
- LeCheminant, A. N. & Heaman, L. M. 1989 Mackenzie igneous events, Canada: Middle Proterozoic hotspot magmatism associated with ocean opening. *Earth planet. Sci. Lett.* **96**, 38–48.
- Lindwall, D. A. 1988 A two-dimensional seismic investigation of crustal structure under the Hawaiian Islands near Oahu and Kauai. *J. geophys. Res.* **93**, 12107–12122.
- Lister, J. R. 1990 Buoyancy-driven fluid fracture: similarity solutions for the horizontal and vertical propagation of fluid-filled cracks. *Fluid Mech.* **217**, 213–239.
- Lister, J. R. & Kerr, R. C. 1991 Fluid-mechanical models of crack propagation and their application to magma transport in dykes. *J. geophys. Res.* **96**, 10049–10077.
- Mahoney, J., Nicollet, C. & Dupuy, C. 1991 Madagascar basalts: tracking oceanic and continental sources. *Earth planet. Sci. Lett.* **104**, 350–363.
- Martin, B. S. 1989 The Roza Member, Columbia River Basalt Group; Chemical stratigraphy and flow distribution. In *Volcanism and tectonism in the Columbia River flow-basalt province* (ed. S. P. Reidel & P. R. Hooper), vol. 239, pp. 85–104. Geological Society of America Special Paper.
- Morgan, J. V., Barton, P. J. & White, R. S. 1989 The Hatton Bank continental margin. III. Structure from wide-angle OBS and multichannel seismic refraction profiles. *Geophys. J. Int.* **98**, 367–384.
- McKenzie, D. P. 1984 A possible mechanism for epeirogenic uplift. *Nature, Lond.* **307**, 616–618.
- McKenzie, D. P. & Bickle, M. J. 1988 The volume and composition of melt generated by extension of the lithosphere. *J. Petrol.* **29**, 625–679.
- McKenzie, D. & O'Nions, R. K. 1991 Partial melt distributions from inversion of rare earth element concentrations. *J. Petrol.* **32**, 1021–1091.
- Oxburgh, E. R. & Parmentier, E. M. 1977 Compositional and density stratification in oceanic lithosphere – causes and consequences. *J. geol. Soc. Lond.* **133**, 343–355.
- Parsons, B. & Richter, F. M. 1981 Mantle convection and the oceanic lithosphere. In *The sea*, vol. 7, *The oceanic lithosphere* (ed. C. Emiliani), pp. 73–117. New York: Wiley.



- Recq, M., Brefort, D., Malod, J. & Veinante, J.-L. 1990 The Kerguelen Isles (southern Indian Ocean): new results on deep structure from refraction profiles. *Tectonophysics*. **182**, 227–248.
- Ritzert, M. & Jacoby, W. R. 1985 On the lithospheric seismic structure of Reykjanes Ridge at 62.5° N. *J. geophys. Res.* **90**, 10117–10128.
- Royer, J.-V., Selater, J. G. & Sandwell, D. T. 1989 A preliminary tectonic fabric chart of the Indian Ocean. *Proc. Indian Acad. Sci. (Earth planet. Sci.)* **98**, 7–24.
- Saunders, A. D. 1985 Geochemistry of basalts from the Nauru basin, Deep Sea Drilling Project legs 61 and 89: Implications for the origin of oceanic flood basalts. In *Initial Reports DSDP 89* (ed. R. Moberley *et al.*), pp. 499–517. Washington, D.C.: U.S. Govt Printing Office.
- Schlich, R. 1982 The Indian Ocean: Aseismic ridges, spreading centres, and ocean basin. In *The ocean basins and margins*, vol. 6, *The Indian Ocean* (ed. A. E. M. Nairn & F. G. Stehli), pp. 51–147. New York: Plenum Press.
- Schmincke, H.-U. 1982 Volcanic and chemical evolution of the Canary Islands. In *Geology of the northwest African Continental Margin* (ed. U. von Rad, K. Hinz, M. Sarnthein & E. Seibold), pp. 273–306. New York: Springer-Verlag.
- Schubert, G. & Sandwell, D. 1989 Crustal volumes of the continents and of oceanic and continental submarine plateaus. *Earth planet. Sci. Lett.* **92**, 234–246.
- Sinha, M. C., Loudon, K. E. & Parsons, B. 1981 The crustal structure of the Madagascar Ridge. *Geophys. Jl R. astr. Soc.* **66**, 351–377.
- Stolper, E. & Walker, D. 1980 Melt density and the average composition of basalt. *Contributions Mineralogy Petrology* **74**, 7–12.
- Tarduno, J. A., Sliter, W. V., Kroenke, L., Leckie, M., Mayer, H., Mahoney, J. J., Musgrave, R., Storey, M. & Winterer, E. L. 1991 Rapid formation of Ontong Java Plateau by Aptian mantle plume volcanism. *Science, Wash.* **254**, 399–403.
- ten Brink, U. S. & Brocher, T. M. 1987 Multichannel seismic evidence for a subcrustal intrusive complex under Oahu and a model for Hawaiian volcanism. *J. geophys. Res.* **92**, 13687–13707.
- Tolan, T. L., Reidel, S. P., Beeson, M., Anderson, J. L., Fecht, K. R. & Swanson, D. A. 1989 Revisions to the estimates of the aerial extent and volume of the Columbia River Basalt Group. In *Volcanism and tectonism in the Columbia River flood-basalt province* (ed. S. P. Reidel & P. R. Hooper), pp. 1–20. Geol. Soc. Amer. Spec. Pap. 239. Boulder, Colorado.
- Watson, S. & McKenzie, D. 1991 Melt generation by plumes: a study of Hawaiian volcanism. *J. Petrol.* **32**, 501–537.
- Watts, A. B. & ten Brink, U. S. 1989 Crustal structure, flexure and subsidence history of the Hawaiian Islands. *J. geophys. Res.* **94**, 10473–10500.
- Watts, A. B., McKenzie, D. P., Parsons, B. & Roufousse, M. 1985a The relationship between gravity and bathymetry in the Pacific Ocean. *Geophys. Jl R. astr. Soc.* **83**, 263–298.
- Watts, A. B., ten Brink, U. S., Buhl, P. & Brocher, T. M. 1985b A multichannel seismic study of lithospheric structure across the Hawaiian-Emperor seamount chain. *Nature, Lond.* **315**, 105–111.
- White, R. R. 1992 Crustal structure and magmatism of North Atlantic continental margins. *J. Geol. Soc.* **149**, 841–854.
- White, R. S. & McKenzie, D. P. 1989 Magmatism at rift zones: the generation of volcanic continental margins and flood basalts. *J. geophys. Res.* **94**, 7685–7729.
- White, R. S., McKenzie, D. & O'Nions, R. K. 1992 Oceanic crustal thickness from seismic measurements and rare earth element inversions. *J. geophys. Res.* (In the press.)
- Williams, L. A. J. 1972 The Kenyan Rift volcanics: a note on volumes and chemical composition. *Tectonophysics*. **15**, 83–96.
- Zucca, J. J., Hill, D. P. & Kovach, R. L. 1982 Crustal structure of Mauna Loa volcano, Hawaii, from seismic refraction and gravity data. *Bull. seis. Soc. Am.* **72**, 1535–1550.